

Pulse

High Current Interrupt Measurement 'HCI'



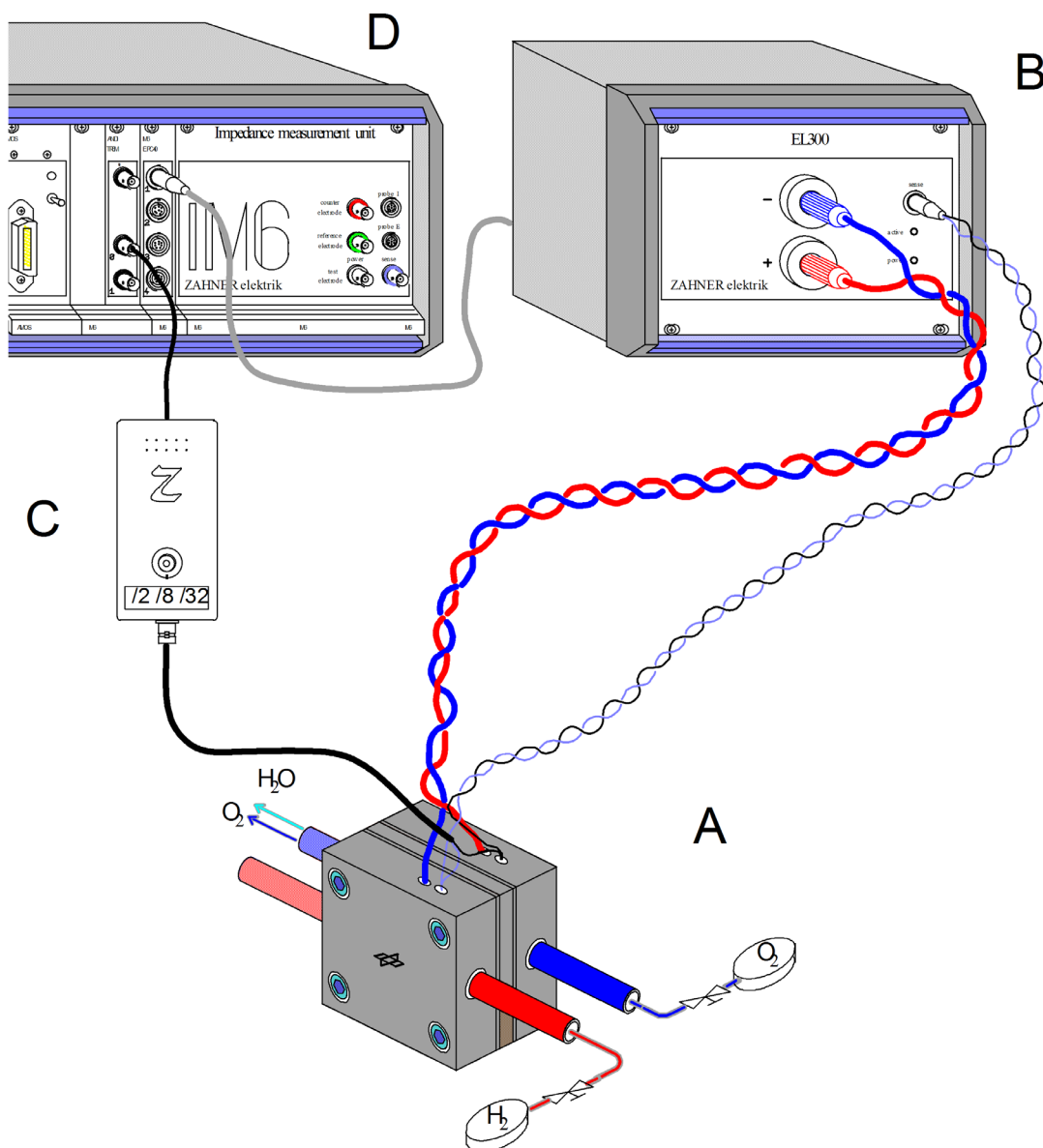
1. Introduction	4
2. Hardware Setup	4
3. Software	5
3.1 Setup of the Current Transient.....	6
3.2 Setup of the Potentiostat Default State	7
3.3 Setup of Trigger Parameters	8
3.4 Setup of Pulse Probe Attenuation.....	8
3.5 Evaluation Control	9
3.6 Initiate an HCl measurement	10
3.7 Export of the Transient	11
3.8 Analysis of HCl measurements	11
3.9 Saving HCl measurements	12

1. Introduction

This manual describes the necessary steps to set up an HCl experiment by means of the Zahner HCl instrumentation. The first part explains how to connect the hardware. Then is described, how the PULSE and the TRC software are to configure, in order to enable and perform HCl measurements. Finally the user is informed about the immediate Ohmic drop determination and how to save and export the data for further analysis.

For a deeper inside into the basics and the technique of HCl, please refer to the attached extract from our EI.Apps. issue 1/2002, p. 1-6.

2. Hardware Setup



Besides of the system under test (A, in the example below sketched as a fuel cell) the experimental setup consists of a Zahner slave potentiostat unit (B), usually an electronic load from the Zahner EL-series. An electrochemical workstation Zennium or IM6, C (operated by a PC, not part of the scheme) acts as a controller and as data procession unit. C is equipped with an EPC42 slave potentiostat controller. The first channel connector of the EPC should be wired to the slave potentiostat used. C

also carries a TR8M transient recorder module, which has to collect the pulse transient data with high time resolution.

The signals from the cell under test are not connected directly to the TR8M. In order to scale down the pulse signals to a level appropriate for the TR8M, a Pulse Probe, D, is wired between measuring object and the CH0 input. The pulse probe also provides galvanic isolation and protects the TR8M from hazardous high energy EMP interferences, typically accompanying HCI measurements.

The slave potentiostat has to establish the default conditions at the cell under test. For potentiostatic control, both the power feeding lines as well as the voltage sensing lines have to be connected, like indicated in the drawing. In a galvanostatic experiment the voltage sensing lines may be omitted in principle, but one should to use the complete wiring for a better control and security.

Electrode of sample	Color of current leading wires EL	Color of sense cable		BNC socket of Pulse Probe
		EL	Pulse Probe	
Positive	Red	Black	Black	Shielding
Negative	Blue	Blue	Blue	Center pin

Due to the unipolar range of an EL slave potentiostat, the cell MUST be connected in a way, that the positive polarity electrode (cathode, the O₂-side of a fuel cell) is connected to the lower (+), and the negative polarity electrode (anode, the H₂-side of a fuel cell) is connected to the upper (-) outlet of the EL (for more details, please refer to the EL manual). This wiring corresponds to a positive load current and a negative rest potential measured.

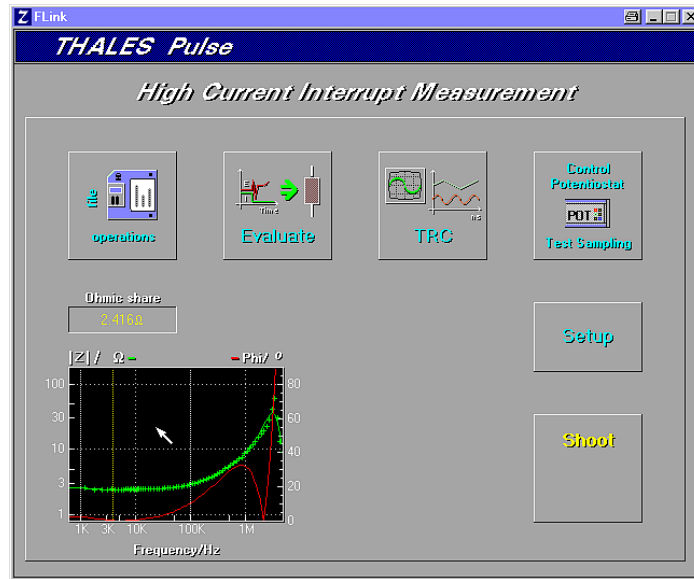
Although the pulse probe provides AC-coupling it should be connected as shown in the picture and table above. Otherwise sign of the transients will swap and the trigger presets in the software will not match.

3. Software

Please enter the PULSE software after activating the “time domain” pop-up menu in the Thales shell:

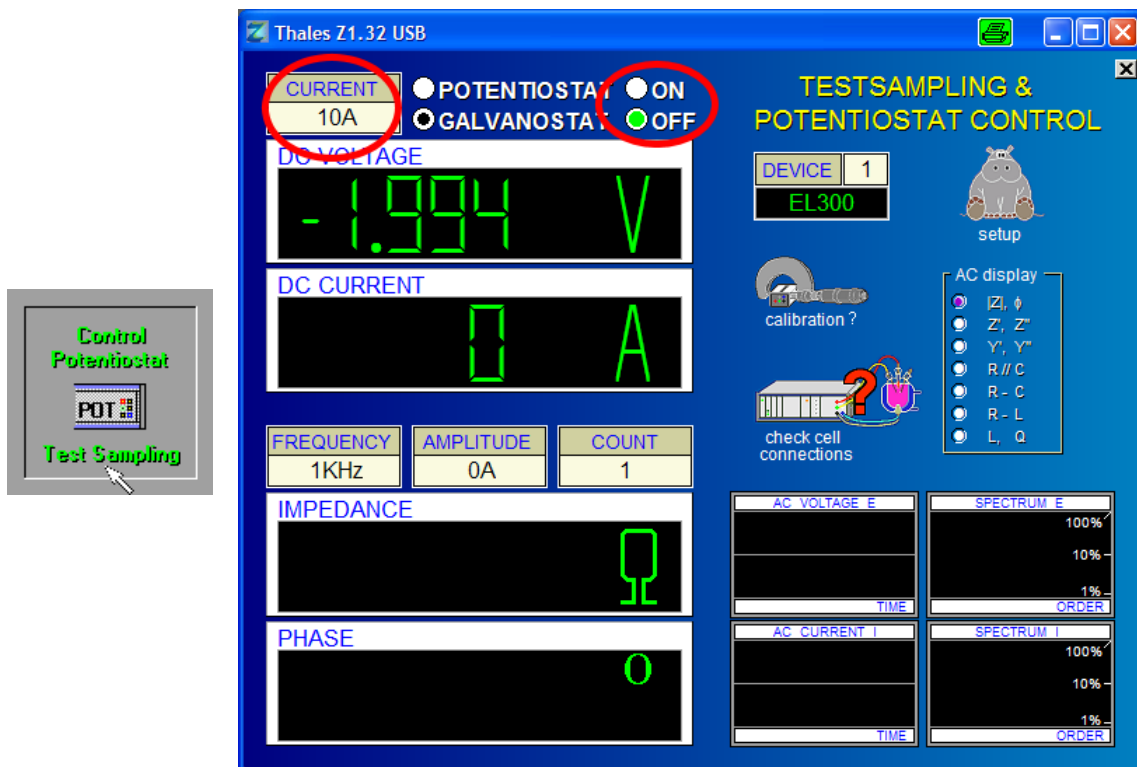


After a successful installation of the HCI hardware arrangement, the PULSE menu is used to trigger a measurement, evaluate the Ohmic drop contribution and save the data for further analysis.



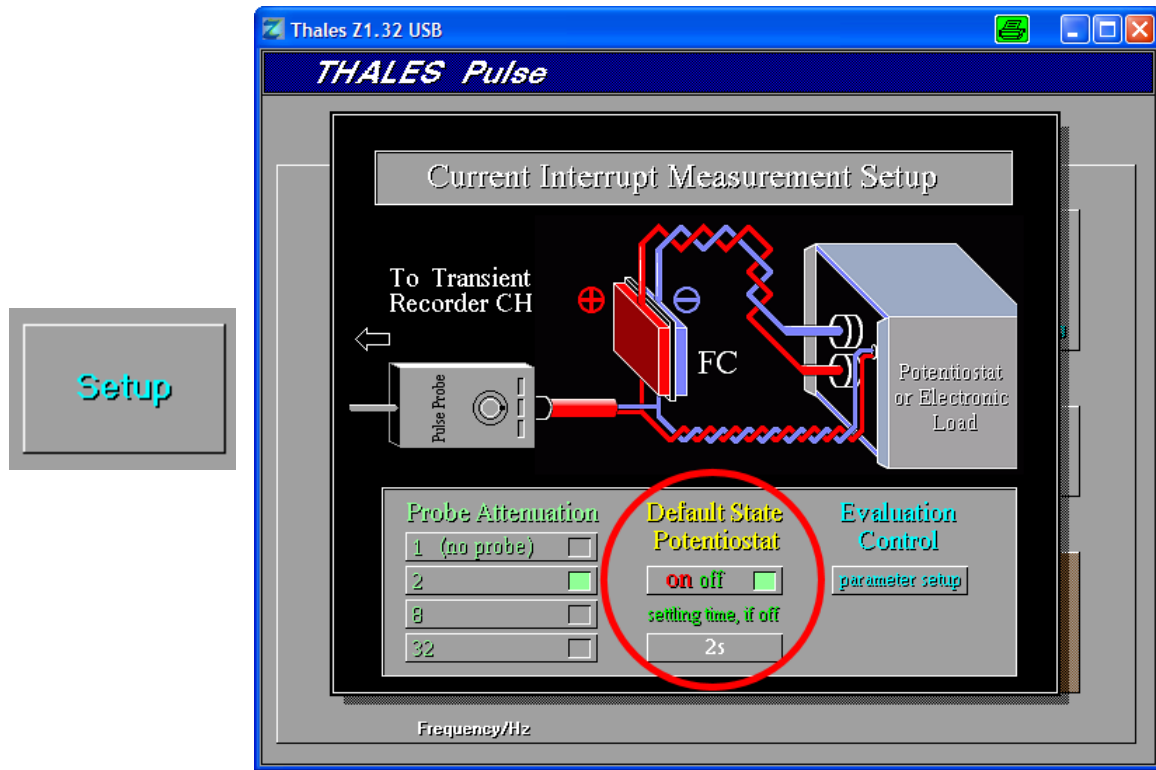
3.1 Setup of the Current Transient

The device and current used for the transient is set by using the control potentiostat button of the Pulse software. Choose the device for the current transient, here EL300 as device 1, and the current, here 10 A. There are two possible default states of the potentiostat. If the potentiostat is switched off, as shown in the picture below, the Pulse software will switch the potentiostat automatically on for a settling time given in the Pulse setup before recording the current interrupt. The other option is to have the potentiostat switched on as default state and only switch it off shortly for the transient measurement. The setting made in the testsampling must correspond to the setup of the pulse as described in chapter 3.2.



3.2 Setup of the Potentiostat Default State

The pulse setup must be configured to match the default state of the potentiostat set in the testsampling. To enter the pulse setup click the setup button in the Pulse main screen.



Toggle between the default states by clicking on the **on/off** button. In case the real state does not match the actually selected one, the HCI-trigger-button “shoot” is disabled.

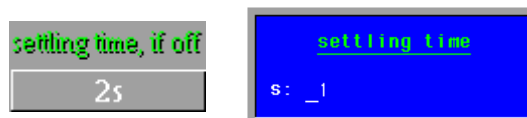
ON  The potentiostat is off for the duration time period of the current interrupt ($\approx 0.2s$). Before and after the pulse it is active (on). This is usually the

Default state for fuel cell HCI measurements.

OFF  The potentiostat is on only during a settling time period just before the current interrupt measurement and is switched off for the rest of the time. This is usually the

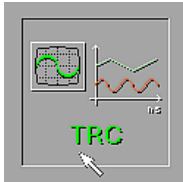
Default state for battery HCI measurements.

The settling time period, active in the “default potentiostat state = off” mode, should normally be chosen just long enough to allow electronic settling (between 0.5s up to some s).



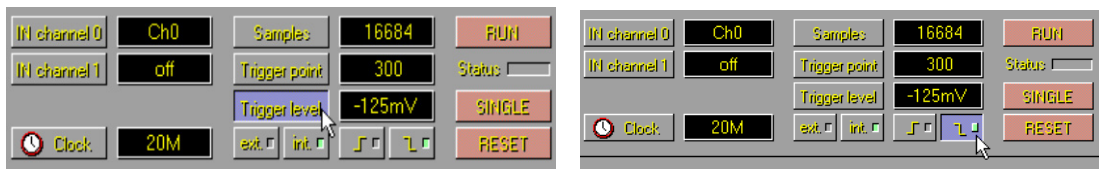
3.3 Setup of Trigger Parameters

Before an HCI measurement can be “shot”, the user should complete the necessary settings of the transient recorder to prepare the instrument for a correct triggering capability. Use the “TRC” entry to enter the transient recorder menu. Please refer to the TRC manual for more details about TRC.



Entering PULSE will pre-configure the transient recorder due to the requirements of HCI, but apart from some triggering adjustments: The optimum triggering conditions usually change with the object under test, with the load conditions and the adjustments of the pulse probe. Therefore the corresponding settings of the transient recorder have to be adjusted accordingly, but:

Do not change any settings in the TRC menu, except trigger level and polarity!



For a correctly connected cell under test, controlled by an EL slave potentiostat, the load current is always positive. An interrupt will therefore cause a current transient into negative direction (from the steady state mean value down to zero). This is accompanied by a potential transient into negative direction. Therefore a negative trigger level as well as a negative trigger slope has to be chosen.

The selection of the level value is not very critical, but nevertheless a little bit more tricky than slope and polarity: for best case accuracy, it should be between 20% to 50% of the Ohmic drop step height expected. Too low (absolutely) level selected may cause spontaneous triggering on noise, too high (absolutely) level will prevent triggering. If you are uncertain, perform some test-shots to find out the best value.



In order to check or change the steady state conditions, one may use the “control potentiostat” entries from both the PULSE as well as the TRC menu.

In a typical HCI measurement condition, the mean (steady state) current should be at least 5 A or higher. The height of the potential pulse one may expect, is the product between the current at the interrupt time (in a fuel cell system usually identical with the steady state current) and the Ohmic contribution. Take 25% of this value as trigger level.

3.4 Setup of Pulse Probe Attenuation

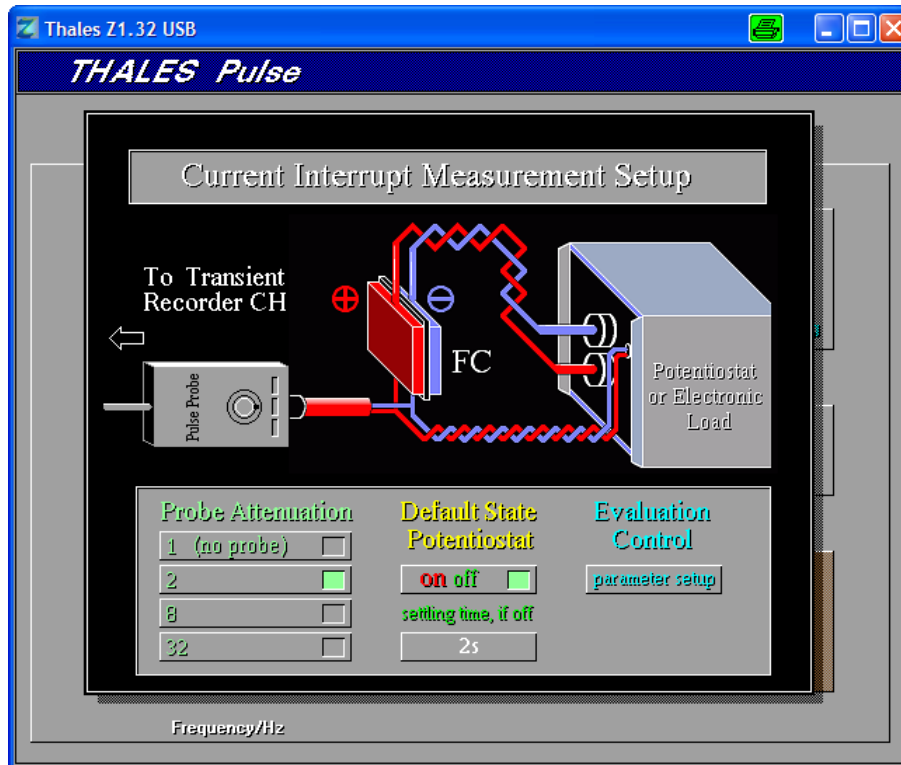
The direct input of the transient recorder allows a dynamic range of $\pm 2V$. The really observed pulse may have a much higher initial amplitude due to overshoot and ringing, depending on the parasitic inductance of the current carrying circuit. This can overload or even damage the inputs of the TR8M. Therefore the pulse probe provides galvanic isolation and attenuation between the sample and the inputs of the TR8M.



In the HCI setup menu the user can select the sensitivity range for the pulse response. Use the more sensitive ranges (for instance /2) for lower current and lower Ohmic drop, for instance state “/2” for single cell fuel cells. Use the less sensitive ranges for instance in fuel cell stack measurements. Otherwise nonlinear clipping of the initial pulse response may reduce the accuracy of the result.

The software cannot check, if the physical state of the attenuator selector fits the state of the HCI setup, therefore:

Be sure, that the HCI setup fits the physical state of the pulse probe!



The signal amplitude is attenuated to the dynamic range of the TR8M in the following manner:

Probe Attenuation

1 (no probe) <input type="checkbox"/>	Direct input to TR8M, no attenuation Dynamic range: ± 2 V, no galvanic isolation.	1 (no probe) <input checked="" type="checkbox"/>
2 <input type="checkbox"/>	Input through Pulse Probe, divisor 2 Dynamic range: ± 4 V, galvanic isolation	2 <input checked="" type="checkbox"/>
8 <input type="checkbox"/>	Input through Pulse Probe, divisor 8 Dynamic range: ± 16 V, galvanic isolation	8 <input checked="" type="checkbox"/>
32 <input type="checkbox"/>	Input through Pulse Probe, divisor 32 Dynamic range: ± 64 V, galvanic isolation	32 <input checked="" type="checkbox"/>

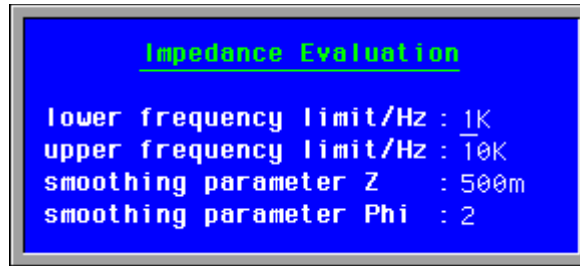
Only for testing purposes!

After changes of the probe sensitivity in the HCI setup it is recommended to control the trigger level.

3.5 Evaluation Control

The HCI measurement setup provides the possibility to edit the parameters for the automatic Ohmic drop calculation. In this process, the frequency range between the "lower frequency limit " and the "upper frequency limit " is analysed. The minimum value of the impedance modulus is taken then as the Ohmic share estimate. Besides this, for the calculation of the scalar impedance spectrum and for the reverse ZHIT transformation (see addendum), leading to a phase angle course approximation, different smoothing operations are used. Normally it is not necessary to change the pre-configured widths of 0.5 and 2 respectively. For very noisy measurements, take "wider" smoothing parameters (according a wide Gaussian weighting window).

When leaving the HCI setup page, the setup data are stored, besides the trigger adjustment information for the transient recorder. The settings will be recalled again after a restart of Thales.



3.6 Initiate an HCl measurement

If all conditions of an HCl measurement are met, the **SHOOT** button gets active. Trigger the HCl measurement by clicking on this button.

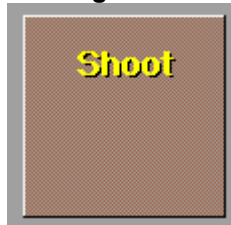
If the **SHOOT** button is not active check:

- State of the potentiostat in testsampling and default state Pulse setup match.
- In case of default on the current is more than 2 A.

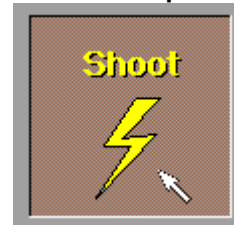
Starting conditions not met



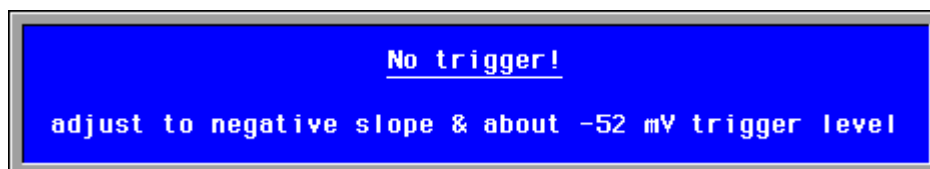
Starting conditions met



Start interrupt measurement

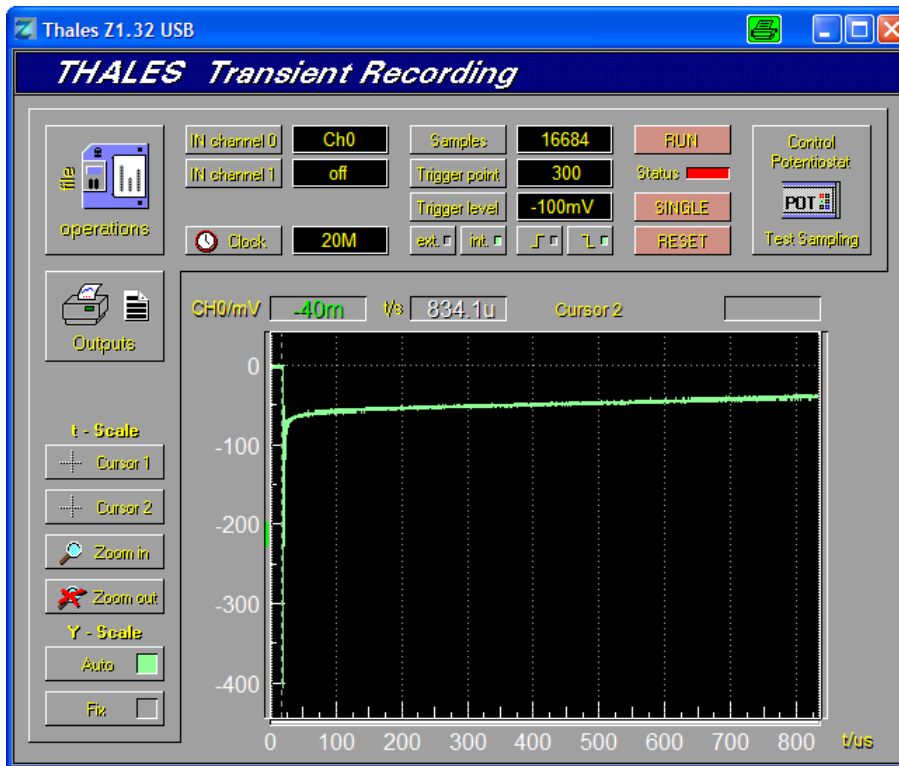


The TRC panel will pop up, displaying an empty graph data section (initially), or the last shot curve graph. The PULSE software will interrupt the cell current for about 0.2s, while the transient recorder waits for a triggering signal. If a wiring problem exists or if the trigger condition settings are not selected properly, no trigger event will take place. A message will pop up, giving a suggestion for the correct trigger level.



Please note this suggestion relies on the correct wiring as described in chapter 2. Otherwise the suggestion will not be correct. After checking the wiring and the trigger settings try another shot from the pulse main screen.

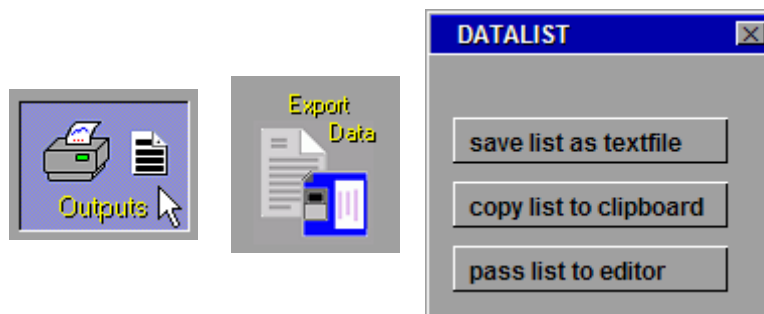
After a successful shot, the resulting curve displayed should exhibit a negative going step function, with the step (trigger event) located around 30 μ s.



Now the transient can be viewed, zoomed, exported etc. in the usual way like described in the TRC manual. By means of the "file operations" menu, the transient raw data can be saved for later analysis. The most effective way for analysis is getting back to the PULSE menu by leaving the TRC panel.

3.7 Export of the Transient

Using the outputs button the transient can be exported either as ASCII text or as graphics. The ASCII text can either be saved on disk as a file, copied to the clipboard or pasted directly to the Thales editor.

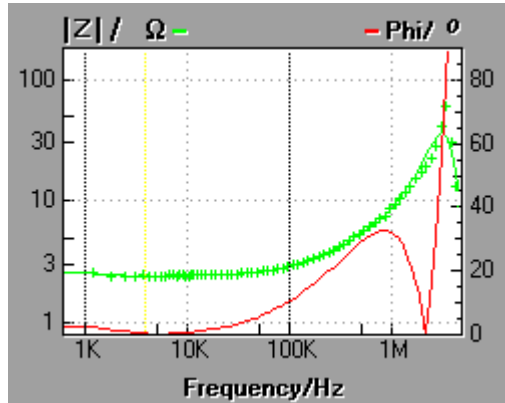


3.8 Analysis of HCI measurements



The PULSE menu provides the possibility for an instant analysis. For details of the analysis process, please refer to the addendum. The evaluation is based on the reconstruction of an impedance spectrum, belonging to the actual pulse response. Assumed, that previously performed calibration measurements are representative for the (un-observed) actual current course within a certain accuracy, the (scalar) impedance spectrum can be calculated from the fourier transform of the observed voltage pulse, divided by the fourier transform of the

normalized current response available from the calibration results. The quotient is then scaled by the current measured at the time just before the interrupt. The spectrum found is examined for the impedance minimum within the frequency range, selected in the setup. This minimum value is then displayed as the Ohmic share estimate.



Scalar impedance spectrum, together with the reconstructed phase angle, found by an inverse ZHIT approximation. The yellow line within the dotted black lines of the frequency limit marks the location of the impedance modulus minimum.

3.9 Saving HCI measurements

An even more precise analysis can be done, if the resulting spectrum is passed to the SIM equivalent circuit simulation and fitting software.



For that, click this button and call the file manager. The calculated impedance spectrum data can be saved. Later on it can be loaded in the usual way into the SIM software for further analysis.

Current Interrupt Technique - Measuring low impedances at high frequencies

F. Richter, Siemens AG, KWU, Erlangen, Germany, franz.richter@erl11.siemens.de

C.-A. Schiller, Zahner-elektrik, Kronach, Germany, cas@zahner.de

N. Wagner, DLR, Stuttgart, Germany, norbert.wagner@dlr.de

If a power generating device is examined, its dynamic electrical equivalence generally will appear as a network which represents anode, cathode, membrane, electrolyte, and connectors.

The specific losses of every partial impedance of the network contribute to the overall efficiency of the device. The porous layers of anode and cathode, responsible for the charge transfer reaction, normally play a major role. Other contributions seem to be much less important. There is the resistance of the electrolyte or the membrane as well as the resistance of contacts and connectors. A dynamic part is added by the inductance of the body and the connectors.

Nevertheless, the ohmic part (electrolyte, membrane, connectors) plays an important role regarding the performance of the device and accounts sometimes for the main part of the overall losses. It is very sensitive to degradation caused by corrosion and thermal stress.

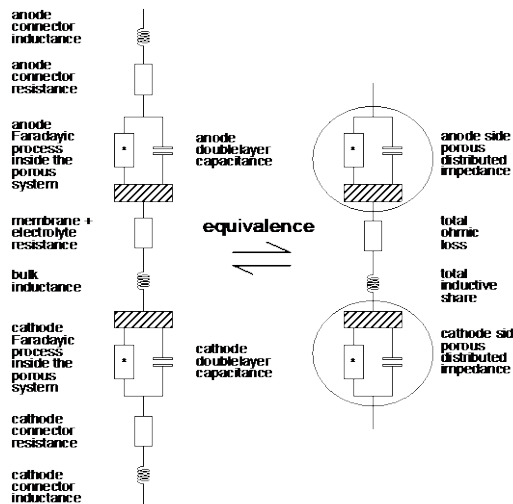


Fig. 1: Simplified electrical equivalent circuit of a typical electrochemical power source device

In applications with dynamic load changes the inductive parts, for example in a laptop computer battery or in electromotive applications, are limiting the maximum pulse load available.

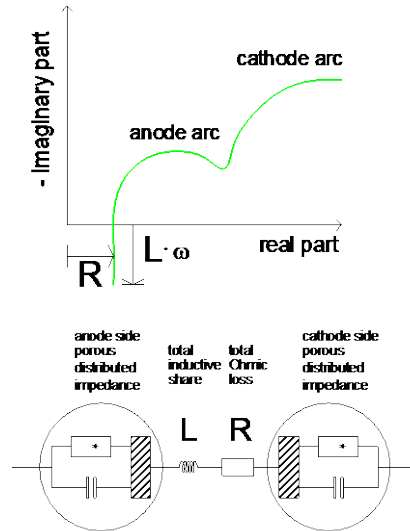
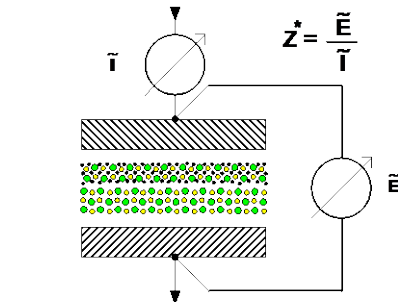


Fig. 2: The appearance of ohmic share and stray inductance in a fuel cell spectrum

EIS allows to separate all contributions and to determine the ohmic part in the high frequency region of a spectrum, where the impedance curve intersects the real axis. The inductance is shown at successive higher frequencies in the diagram. But there is one great restriction: Measuring impedance always means to measure two signals, current and voltage.



$Z =$ Impedance of the Object of Interest
With the Extensions in Space x, y, z

$$E_{\text{noise}} \propto \omega, x, y, z, \vec{I}$$

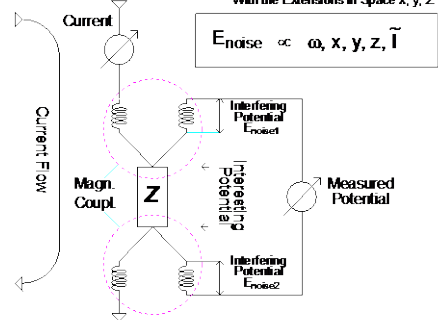


Fig. 3: Basic impedance measurement circuit – principle (top) and detail (bottom)

A closer look at the circuit in figure 3 shows that the potential information does not only contain the interesting part from the site of the connecting terminals. It is rather contaminated by dynamically induced error voltages. These errors are caused by unavoidable mutual induction from the magnetic field of the current circuit.

The interference increases with increasing frequency and with the strength of the magnetic field of the current. It depends on the geometry and grows with the dimensions of the object. For the investigation of power sources this means: The more you scale up, the lower is the available upper frequency limit (f_g). Finally, there is a limit for the EIS at low ohmic objects. At a rough estimation you can calculate with:

$$f_g \approx 1 \text{ MHz} * |Z|_{\min} / \text{Ohm}$$

As a consequence, the window for getting an Ohmic resistance information by means of the EIS gets smaller for bigger cells. For certain systems, the window will be closed.

What can be done to complement the EIS under these conditions? The question is answered by the well known current interrupt technique, which does not need the knowledge of two signals simultaneously. The principle is depicted in figure 4 and explained in the following:

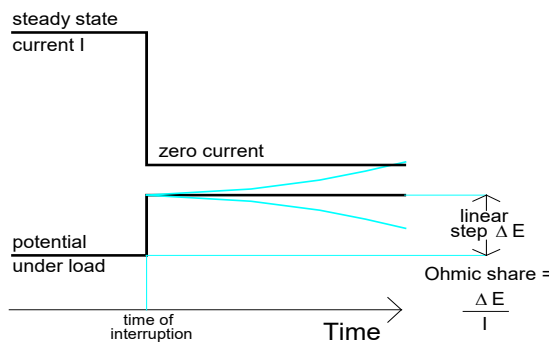
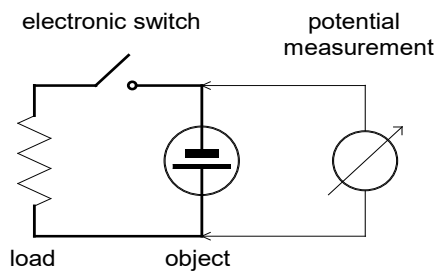


Fig. 4: Principle of current interrupt technique to determine the ohmic share

A steady-state current is interrupted by a switch. The step response of the potential is sampled and analysed assuming that the current drops instantaneously from its stationary value to zero.

In practice, the settling time depends on the electromagnetic energy stored in the parasitic capacity and inductivity of the cell arrangement on the one hand and the damping process on the other hand. Provided that the set-up is built appropriate,

the interruption results in a breakdown of the current to at least small values within a short time. In this case, the potential will be disturbed much less by mutual induction compared with an EIS measurement.

In theory, the ohmic contribution to the overall impedance can be easily seen from the height of the fast rectangular step of the potential. For the evaluation a linear step model is commonly used.

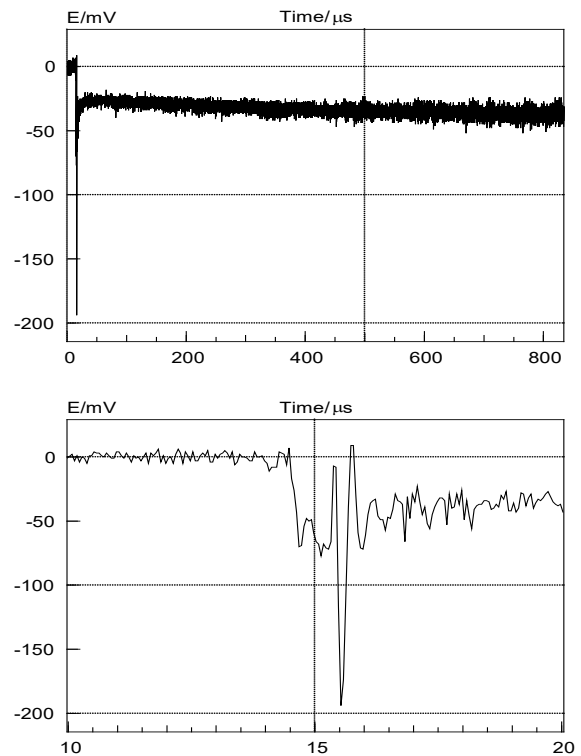
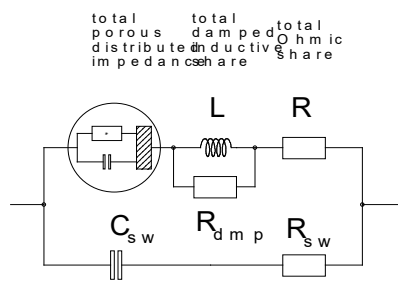


Fig. 5: Typical current interrupt potential step response. Long (top) and short (bottom) term response of a single cell PEM fuel cell at 80 A.

But this evaluation suffers from the fact that the analysis of the time domain data is interfered by the "ringing" in the signal as a result of the parasitic resonance. In addition, the early phase of the response is characterized by a non-linear behavior due to the imperfect characteristics of the electronic switch. Furthermore, the response of both double-layers may follow soon after the interruption when the concentrations of the involved species turn from their steady state values to new ones without load. All these effects bend and distort the expected ideal shape of the potential step. Therefore, the automatic analysis of pulse measurements by means of a simple fit to a linear step model often leads to inaccurate results.

Our aim was to improve the method in order to get results of comparable reliability to the EIS. The basic idea is not to evaluate the distorted step function in the time domain. Instead, after a transformation of the data into the frequency domain, the resulting spectrum and all parasitic effects can be analysed by means of EIS methods.



C_{sw} : Capacitance and resistance of the electronic switch
 R_{sw} : Resistance of the electronic switch
 L : Integral inductance
 R_{dmp} : Damping of the inductive share due to the parasitic effects of the switch circuit
 R : Ohmic share of the electrochemical cell

Fig. 6: Approximate equivalent circuit for a complete high current interrupt measurement set-up of an electrochemical power source device.

In figure 6, a simplified equivalent circuit for a complete HCI measurement set-up of a power cell is shown. It contains the impedance of the active cell part (circle), the integral inductance (L) and resistance (R) and the parasitic effects of the switch circuit. The resonance circuit is mainly built of the series inductance, the double layer capacity and the capacity of the electronic switch. It is responsible for the overshoot and "ringing" in the pulse response signal.

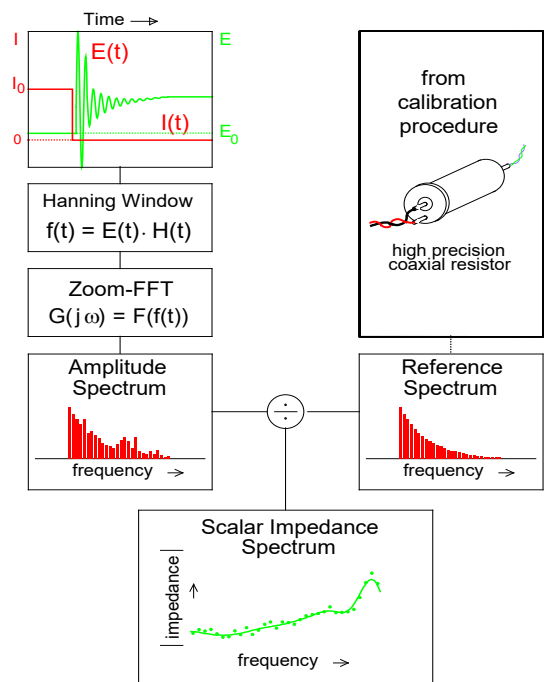


Fig. 7: Principle scheme of the Zahner high current interrupt data processing.

Figure 7 illustrates the essential steps for the transformation of the time domain data into the frequency domain. The potential response signal E is sampled by a transient recorder. The numeric algorithms use discrete Fourier transform methods to achieve an effective analysis. In order to minimize the errors caused by their application on single events, a weighing function has to be applied. At least, a *Zoom FFT* calculates the amplitude spectrum in the frequency domain. A similar procedure using a reference resistor was done for calibration. The quotient of both spectra finally leads

to the modulus of the impedance of the unknown object.

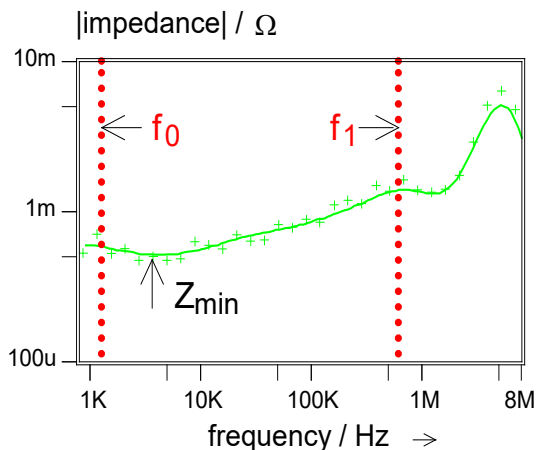


Fig. 8: Automatic evaluation of the ohmic share from the scalar impedance function.

This scalar impedance spectrum can be used to evaluate the ohmic share in a simple, automated way: The user selects a reliable frequency range for analysis, which excludes the parasitic resonance at the high frequency end. The impedance minimum within this range represents the ohmic share with an acceptable accuracy of about 1 to 3%.

If you want to evaluate the response spectrum with the standard methods of the EIS, beside the impedance, the phase data will be necessary: For this calculation a relation between impedance and phase for all two pole impedance objects of minimum phase can be used. The ZHIT¹ relation allows to calculate the modulus of the impedance course from the course of the phase angle. It will also be able to perform the inverse application, if one uses the ZHIT in an iterative numeric way. This is the way, our analysis software obtains a complete spectrum.

The complex spectrum can now be analyzed in the usual way, for instance, by means of simulation and fitting of the equivalent circuit. According to our experience, the ohmic share can be determined in this way, with typically the double or triple accuracy compared to the automatic minimum detection in the scalar impedance function.

Figure 10 is a sketch of the practical set-up of our high current interrupt measurement arrangement of a fuel cell. The electrochemical cell (A) is supplied by means of an electronic load (B) or another type of high power potentiostat to force the steady state load conditions. Additionally, the potentiostat acts as fast electronic switch for the current interruption.

¹ W. Ehm, R. Kaus, C.-A. Schiller, W. Strunz: ZHIT - a simple relation between impedance modulus and phase angle... Electrochemical Society Proceedings 2000-24, 1

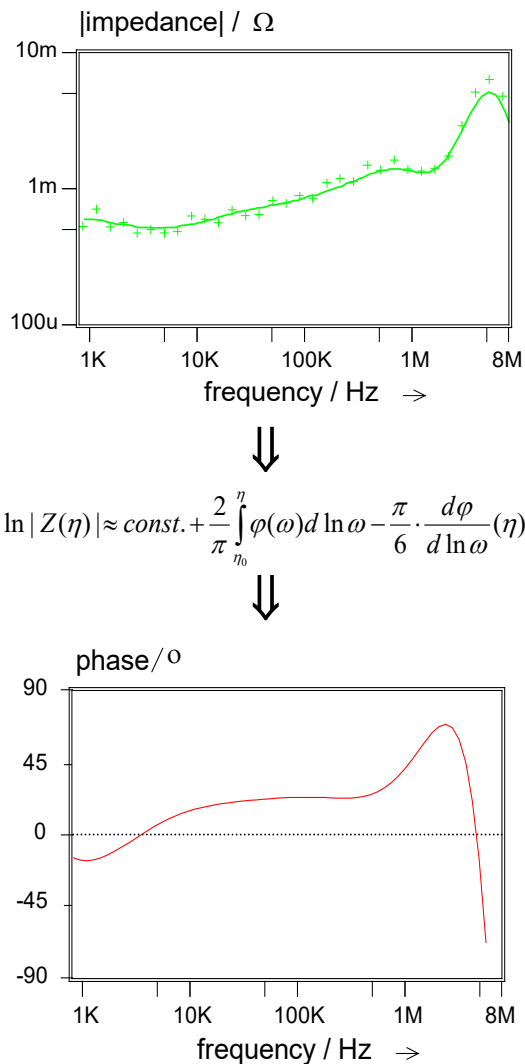


Fig. 9: Calculation of the phase angle from the impedance modulus by means of the inverse application of the ZHIT¹ transform. The ZHIT equation shows that the impedance modulus at the frequency η can be calculated from the integral of the phase angle course $\varphi(\omega)$ within limited frequency boundaries (η_0 to η). A correction term proportional to $d\varphi/d\ln\omega$ enhances the accuracy.

The potentiostat is controlled by an electrochemical workstation (D) including a high resolution transient recorder. The recorder input is connected to the potential sense lines of the cell along a so called pulse probe (C). The main task of the pulse probe is the galvanic isolation of the potential sense circuit from the instrument in order to minimize electromagnetic interference. On the other hand, it is responsible for the protection of the instrument input by means of an energy consuming clipping circuit.

After a short 'sampling shot' during the interrupt, the instrument switches on the current again, in order to re-establish the steady state and to avoid potential damage of the cell. The pulse response is analyzed then by the software of the workstation as described before.

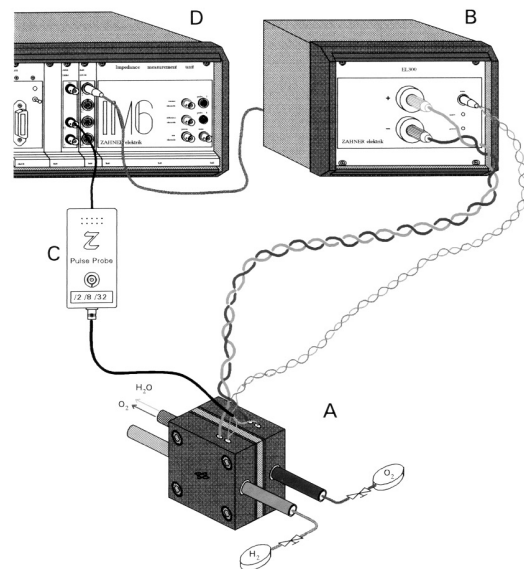


Fig. 10: Practical set-up of a high current interrupt fuel cell measurement arrangement

A lot of test experiments under controlled conditions have been done. The major experience is that, compared with the standard EIS, the HCI is much less sensitive to mutual induction artefacts. This is illustrated by the example depicted in figure 11. Here, we made test measurements at resistors using two different, intentionally non-optimized connection geometries. As you can see, the strong in-phase mutual induction of the above example leads to an inductive component which seems unrealistically high in the case of the standard EIS. The HCI method, however, leads to the almost exact value.

With the other example, which shows a strong out-of-phase mutual induction, one obtains almost the same impedance functions, which has been omitted here. Yet, the phase diagram shows paradox behaviour for the standard EIS curve: The course indicates capacitive characteristics! The phase curve of the HCI experiment shows the correct sign due to its origin from the ZHIT transform.

We also found that the HCI worked fine with power generating devices. As an example, the results of an EIS and a HCI experiment at a high temperature fuel cell are depicted in figure 12. The cell has been driven with air and humidified hydrogen and generated more than four Amperes at a potential exceeding 0.73 Volts. In both experiments the best case wiring was used to reduce the mutual induction contribution.

The original HCI potential step response is plotted on top of figure 12. At the bottom, the transformed impedance (circles) as well as a comparative impedance measurement (rhombi) are drawn. As one can see, the methods complement each other for the different frequency ranges. In this special case, the frequency limit for the EIS experiment to get accurate information on the ohmic share is not exceeded. Therefore, both methods deliver the correct results.

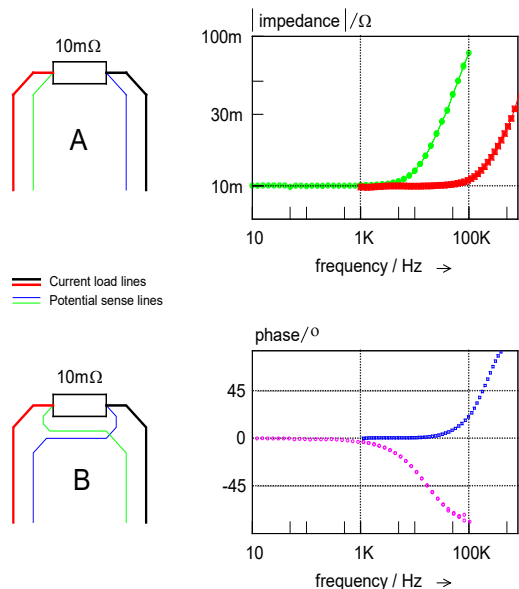


Fig. 11: Results of test measurements at reference resistors incl. mutual induction (MI) components.
 A: In phase MI leads to a high inductive response in the case of EIS (full dots) whereas the HCI spectrum (squares) matches the theory.
 B: Out-of-phase MI causes paradox capacitive (-) EIS phase courses (squares) while the HCI phase course shows the correct phase sign for inductance (+).

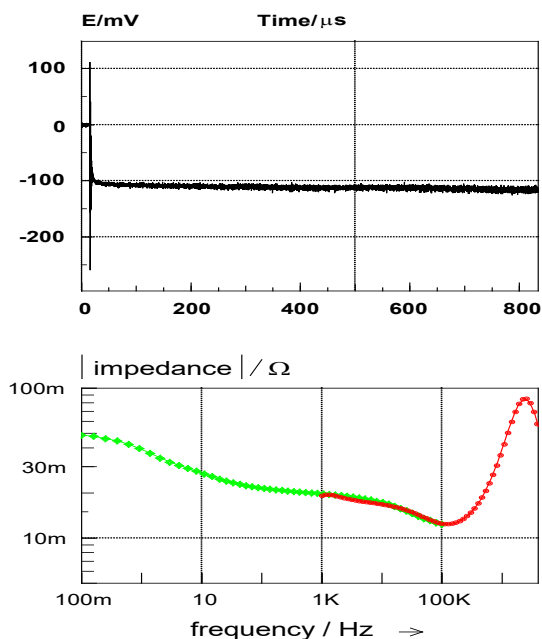


Fig. 12: High current interrupt measurement of a single solid oxide fuel cell at 866°C.
 EIS: 100 mHz – 100 kHz (rhombi)
 HIC: 1 kHz – 800 kHz (circles)

The last example demonstrates that the dominating error from the unavoidable mutual induction falsifies the result of standard EIS measurements at very low impedance objects. In the experiments depicted in figure 13, a HCI measurement (top) as well as a comparative EIS measurement (bottom, triangles)

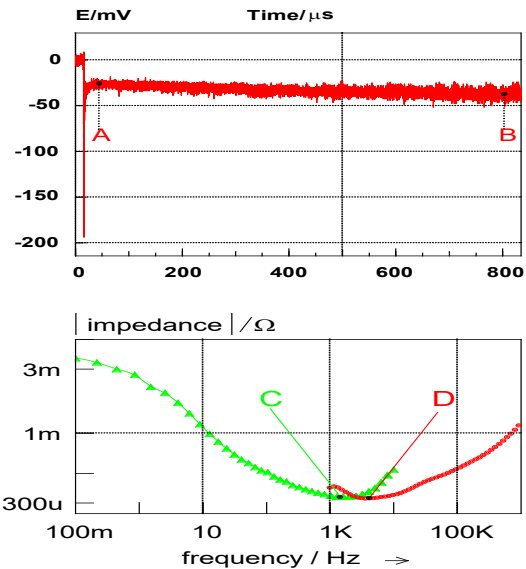


Fig. 13: High current interrupt measurement of a single PEM fuel cell at 85° C and 80 A. The resulting spectrum (C) is compared with a standard EIS (D).

on a big PEM fuel cell at a current of 80 A were performed. The shift of the increase of the impedance for the transformed HCI-data (circles) to higher frequencies indicates the smaller sensitivity of the HCI measurement against the mutual induction.

In our opinion, the missing correspondence between the EIS- and the HCI-data at the low frequency end of 1.1 KHz results from a non-linear component in the long term pulse response signal. HCI analysis has to rely on the rule of linearity. The transient changes of about -10 mV within the 0.85-millisecond-analysis-interval may be enough to violate this rule.

Conclusion

1. EIS capabilities are basically limited by mutual induction at the high-frequency low-impedance edge. This falsifies significantly the results for ohmic and inductive share.
2. The HCI capability is limited by the magnetic energy stored in the load circuit.
3. The HCI analysis can be automatically analyzed reliably by transforming the time data into the frequency domain.
4. According to our experience, HCI can extend the available frequency range about a factor of three to ten in a carefully optimized experimental set-up.
5. HCI data interpretation should not be extended to the low frequency response. The unavoidable violation of the EIS linearity rule after a certain interruption time may lead to misinterpretations.
6. Thus, an arrangement which performs both, the standard EIS and the HCI measurement within one set-up, is the best choice for the challenges of electrochemical power source device testing.

